MAGNETIC RESONANCE IN MEDICINE 14, 187–193 (1990)

Time-of-Flight Effects in MR Imaging of Flow*

FELIX W. WEHRLI

Hospital of the University of Pennsylvania, 3440 Market Street, Suite 420, Philadelphia, Pennsylvania 19104

Received December 19, 1989

This article provides a brief overview of one of the two fundamental physical principles which lead to a modulation of the magnetic resonance signal of moving spins: the time-of-flight effect. It then discusses some of its characteristic manifestations in spin-echo imaging and reviews strategies for exploiting the effect to quantitate vascular flow.

FLOW PHENOMENOLOGY

The vascular signal intensity in MR images can assume almost any conceivable shade of gray, from the highest theoretical signal corresponding to full spin polarization down to background intensity, thus making it a bewilderingly complex phenomenon. Vessel orientation, flow velocity and its intraluminal distribution, as well as the specific pulse sequence used, all critically affect signal intensity. In conventional 2D FT spin-echo imaging vessels running in the imaging plane, with few well understood exceptions, usually appear with very nearly background intensity. By contrast, for vessels transecting the imaging plane at some angle $\alpha > 0$, a phenomenon first denoted "paradoxical enhancement" (*1*), but now more commonly referred to as "flow-related enhancement" (see, for example, (*2*)), may occur, provided a substantial fraction of spins without an RF history are present at the time of excitation. Flow-related enhancement and signal loss are typically caused by inflow/outflow processes, summarized under the term "time-of-flight" effects, which are the subject of this overview. An understanding of this effect is important as it has implications for clinical diagnosis of vascular disorders and also because it is the basis for such imaging options as spatial presaturation (*3*) as well as for some of the most commonly used MR angiographic techniques (*4, 5*).

A significant complication is the circumstance that the observed signal manifestations are usually a composite of the two basic effects encountered in MR imaging of flowing spins: *time-of-flight* and *phase effects*. The latter arise from spins flowing in the direction of a magnetic field gradient, in which case a phase advance or retardation ensues (*6*). In modulus displays the latter can affect signal intensity if a *distribu-*

* Presented at SMRM Workshop on MR Imaging of Blood Flow, Philadelphia, PA, March 13 and 14, 1989.

0740-3194/90 $3.00

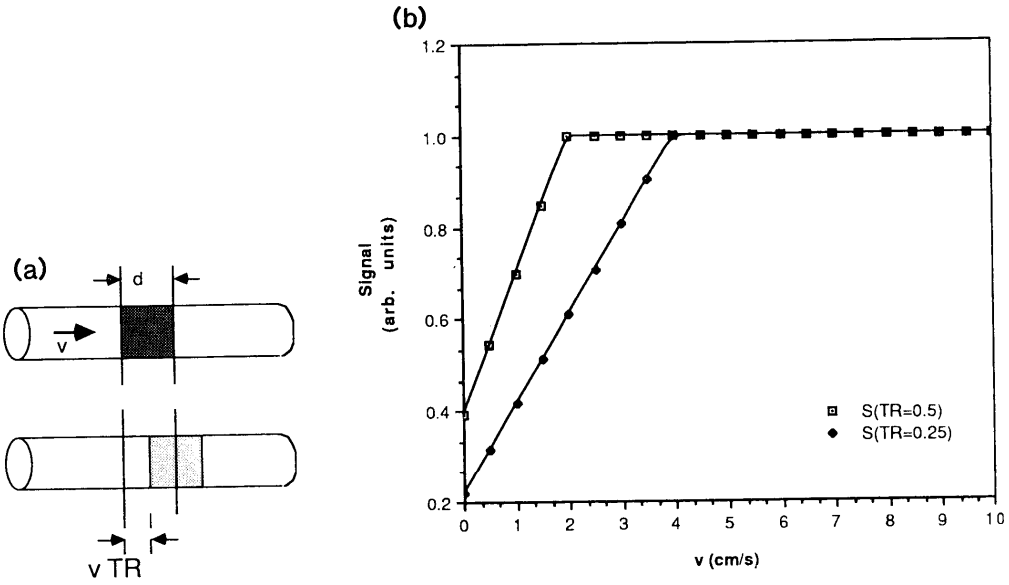

FIG. 1. Time-of-flight effect for plug flow perpendicular to the imaging plane for a series of equidistant 90° RF pulses; (a) spin populations at time $t = 0$ and $T = TR$; (b) signal vs velocity diagram for two pulse repetition times of 0.25 and 0.5 s, a section thickness of 1 cm, and assuming a fluid T1 of 1 s.

tion of velocities across the imaging voxel, as a result of shear or turbulence, is present (*7, 8*). In this case destructive interference of spin isochromats causes signal attenuation. Signal reductions also occur as a result of view-to-view variations of velocity during the cardiac cycle, in which case phase modulation ghosting ensues.

INFLOW/OUTFLOW EFFECTS

The principle of time-of-flight effects was reviewed several years ago by Axel (*9*). More recently Gullberg *et al.* (*10*) and Gore *et al.* (*11*) modeled the signal on the basis of the Bloch equations for a variety of pulse sequence schemes for both plug and laminar flow.

The basic principle is straightforward. Let us assume the conceptually simplest case of spins moving perpendicular to a plane while being subjected to a train of equidistant slice-selective 90° RF pulses, administered every TR milliseconds. It is readily seen that, provided $v < d/TR$, where v is the flow velocity and d the section thickness, two populations of spins are contributing to the signal: a fraction $v \cdot TR/d$ of maximum signal M_{max} and a second fraction $(1 - v \cdot TR/d)$ of signal $M_{max}[1 - \exp(-TR/T1)]$, as illustrated in Fig. 1.

In a plot versus velocity, the signal is found to first increase and then reach a plateau, once all saturated spins have been washed out during the TR period, i.e., for the condition $v = d/TR$.

The next level of sophistication involves the presence of a slice-selective 180° refocusing pulse, applied TE/2 milliseconds after the 90° pulse. Since TE ≪ TR usually

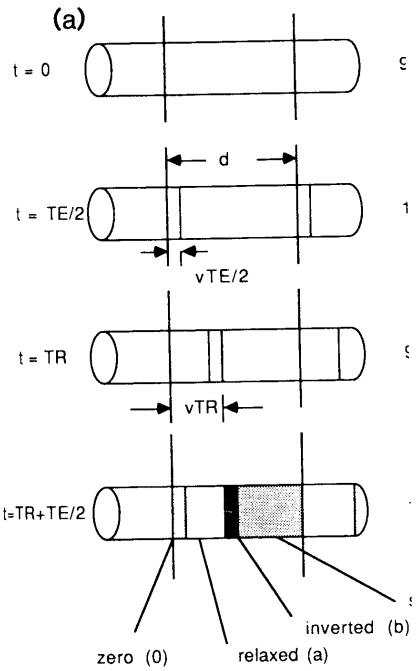

FIG. 2. (a) In the slow-flow regime fou
echo imaging, on the assumption that a s
calculated signal for laminar flow (adapte

holds, the signal behavior for slc
from that discussed for 90° pulse
cant fraction of spins that have
These spins have no transverse
echo. Therefore, the signal will e
reaching background levels for tl
ment of those spins which have b

A detailed analysis shows tha
2a). Let us assume that at time t
then follow this bolus as it adva
time the 180° pulse following th
advanced a total distance v(TR
history have entered the slice. Th
lations are readily determined by

(0) (zero transverse magne
(a) (fully relaxed spins)
(b) (inverted spins)
(c) (saturated)

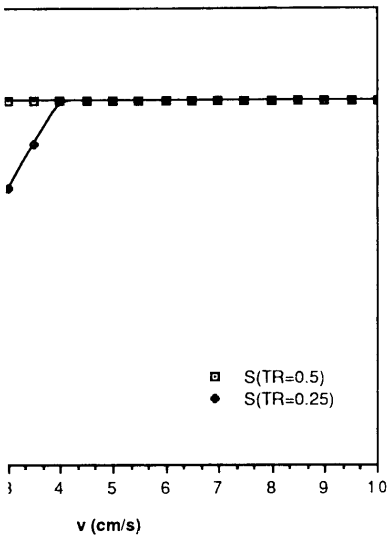

maging plane for a series of equidistant
signal vs velocity diagram for two pulse
assuming a fluid T1 of 1 s.

)f shear or turbulence, is present
chromats causes signal attenua-
v-to-view variations of velocity
tion ghosting ensues.

CTS

l several years ago by Axel (*9*).
11) modeled the signal on the
equence schemes for both plug

e the conceptually simplest case
; subjected to a train of equidis-
y TR milliseconds. It is readily
city and d the section thickness,
al: a fraction $v \cdot TR/d$ of maxi-
) of signal M_{max} [1 − exp(−TR/

: increase and then reach a pla-
during the TR period, i.e., for

ce of a slice-selective 180° refo-
' pulse. Since TE ≪ TR usually

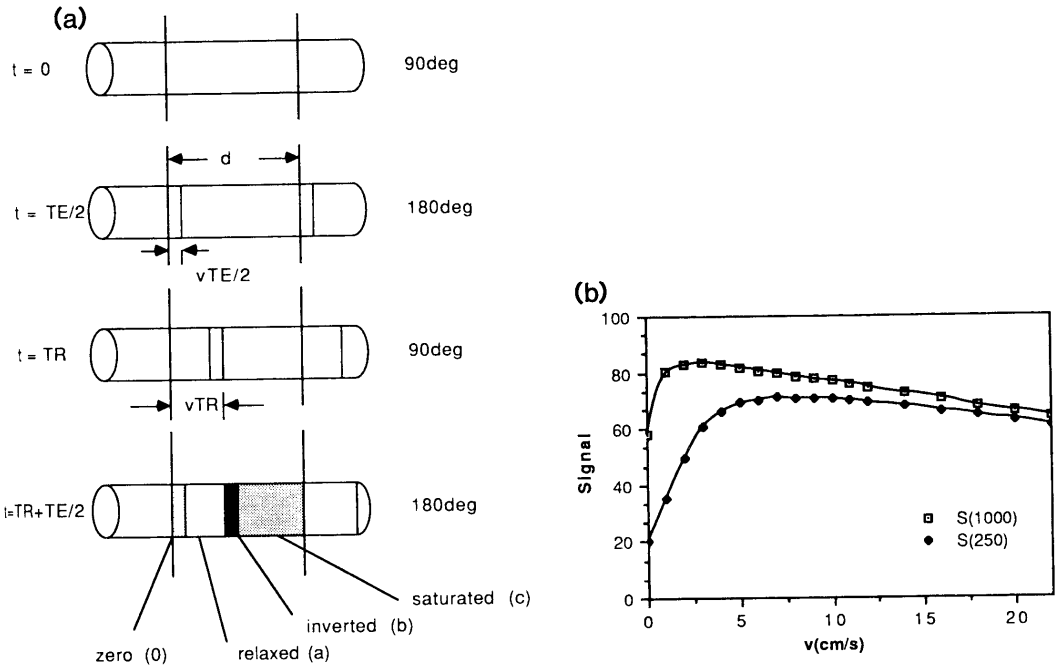

FIG. 2. (a) In the slow-flow regime four populations with different history can be distinguished in spin-echo imaging, on the assumption that a single slice is imaged with both RF pulses being slice-selective; (b) calculated signal for laminar flow (adapted from Ref. (*10*)).

holds, the signal behavior for slow flow velocities ($v < d/TR$) is not much different from that discussed for 90° pulses only. However, as the velocity increases, a significant fraction of spins that have not seen the 90° pulse may enter the imaging slice. These spins have no transverse magnetization and hence do not contribute to the echo. Therefore, the signal will eventually decrease as the velocity increases further, reaching background levels for the condition $vTE/2 = d$, i.e., for complete displacement of those spins which have been excited by a 90° pulse.

A detailed analysis shows that up to four different populations can coexist (Fig. 2a). Let us assume that at time $t = 0$ a 90° pulse is applied, labeling a bolus. We can then follow this bolus as it advances with time. At time $t = TR + TE/2$, i.e., at the time the 180° pulse following the second 90° pulse has been applied, the bolus has advanced a total distance $v(TR + TE/2)$. At this time "new" spins with a different history have entered the slice. The relative fractions of the four distinguishable populations are readily determined by reference to Fig. 2a:

(0) (zero transverse magnetization)	$vTE/(2d)$
(a) (fully relaxed spins)	$v(TR - TE/2)/d$
(b) (inverted spins)	$vTE/(2d)$
(c) (saturated)	$v(TR + TE/2)/d$.

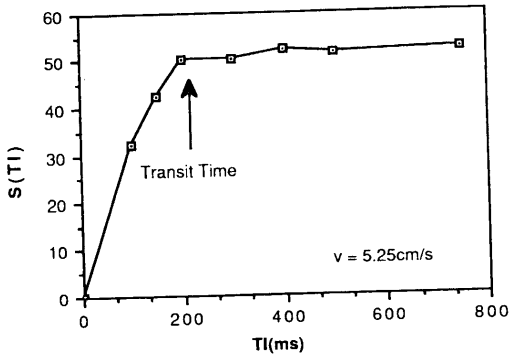

FIG. 3. Washout curve for the femoral vein, determined from ROI signal intensities pertaining to saturation recovery images obtained with different values of the interpulse interval TI (adapted from Ref. (*14*)).

The signal intensities for the three signal-carrying populations labeled a, b, and c can readily be calculated from the Bloch equations:

(a) relaxed $M_0\exp(-\mathrm{TE}/T_2)$

(b) inverted $M_0\{1-2\exp[-(\mathrm{TR}-\mathrm{TE}/2)/T_1]\}\exp(-\mathrm{TE}/T_2)$

(c) saturated $M_0\{1-2\exp[-(\mathrm{TR}-\mathrm{TE}/2)/T_1]+\exp(-\mathrm{TR}/T_1)\}\times\exp(-\mathrm{TE}/T_2)$.

Of course, all four populations are present only provided that $v < d/(\mathrm{TR}+\mathrm{TE}/2)$, i.e., for sufficiently slow flow. The degree of flow-related enhancement or signal reduction, respectively, therefore depends on the flow velocity (i.e., its value relative to d/TR). It is obvious that as v increases population c (saturated spins) will first be displaced and population a (fully magnetized spins) will become dominant. However, eventually, population a will be displaced as well and population 0 (zero signal) will prevail, for which condition a flow void is obtained.

More realistic than plug flow, of course, is a distribution of flow velocities, e.g., laminar flow. Above considerations, valid for plug flow, can be extended in a straightforward manner. A calculated signal–velocity curve for the assumption of laminar flow is displayed in Fig. 2b.

The inflow–outflow effects for laminar flow result in a radial dependence of the signal intensity. In cross-sectional images the signal is predicted to first increase centrally as the flow velocity increases, followed by a central signal loss (due to the predominance of the outflow effects), while peripherally the signal still grows. These effects have been observed in phantoms and during diastolic vascular flow (*12*).

FLOW QUANTITATION

Attempts to measure flow velocity by exploiting the TOF effect are plentiful (*12–18*). The conceptually simplest approach makes use of a two-pulse tag–detect sequence (*12–14*). In this method, tagging of a bolus of spins occurs by means of a selective saturation or inversion pulse ($\alpha = 90°, 180°$), followed TI milliseconds later by a 90° detection pulse. The 90° tagging pulse, typically, is followed by a spoiler gradient which disperses transverse magnetization. Figure 3 (*14*) shows a washout

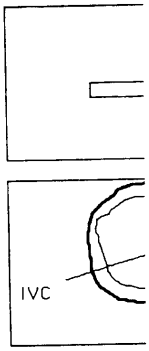

FIG. 4. Principle of the biplanar bolu
the flow direction while the signal is rea

curve for the femoral vein wh
interpulse interval TI. From su
mean flow velocity determined.

The signal from stationary
niques. If a second data set is a
a manner that it encompasses,
the vessel, an image is obtaine
from that obtained with selecti
tionary background is obtained

Gradient echoes are preferab
ure of the spins to experience b
ing the flip angle of the taggin
from stationary spins can effec
subtract two data sets.

An interesting extension of t
180° pulse in a slice-selective sp
if the spacing Δd between excit
condition $v = \Delta d/(\mathrm{TE}/2)$. Th
if multiple echoes are generate
maximum when $\Delta d = (2n - 1$

None of these methods are
bration or the acquisition of mu
as shown in Fig. 3, typically ir
(*15*). A direct measurement, h
lar to the slice-selection plane
applying the slice-selection anc
direction of flow.

When incorporated into a c
the generation of multiple ima
of the cardiac cycle (*20*). From

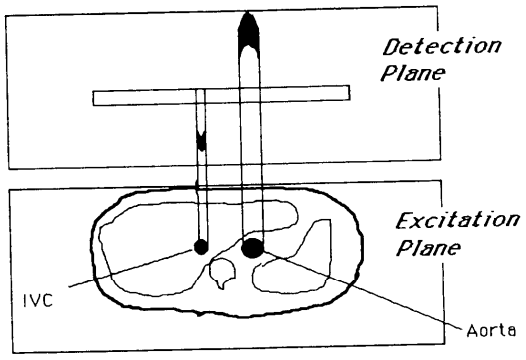

FIG. 4. Principle of the biplanar bolus tracking technique: spins are excited in a slice perpendicular to the flow direction while the signal is read out in flow direction.

curve for the femoral vein where the ROI signal was plotted as a function of the interpulse interval TI. From such curves the transit time can be estimated and the mean flow velocity determined.

The signal from stationary material can be suppressed using subtraction techniques. If a second data set is acquired with the tagging pulse being selective in such a manner that it encompasses, besides the imaging section, the upstream portion of the vessel, an image is obtained with low vascular signal. By subtracting this image from that obtained with selective tagging pulses, a flow image unencumbered by stationary background is obtained (*14*).

Gradient echoes are preferable, since in this case no signal losses occur due to failure of the spins to experience both 90° and 180° pulses (*15*). By appropriately selecting the flip angle of the tagging pulse, it has been shown that the steady-state signal from stationary spins can effectively be suppressed (*16*), thus obviating the need to subtract two data sets.

An interesting extension of the tag–detect principle is to displace downstream the 180° pulse in a slice-selective spin echo (*17*). In this case, maximum signal is obtained if the spacing Δd between excitation slice and detection slice (180° pulse) satisfies the condition $v = \Delta d/(\mathrm{TE}/2)$. The velocity range which can be studied can be extended if multiple echoes are generated. It is readily seen that for the nth echo the signal is maximum when $\Delta d = (2n - 1)(\mathrm{TE}/2)v$.

None of these methods are clinically practical as they require either velocity calibration or the acquisition of multiple images for the establishment of a washout curve as shown in Fig. 3, typically in conjunction with the use of curve fitting techniques (*15*). A direct measurement, however, is possible if the signal is read out perpendicular to the slice-selection plane (*18–20*), as illustrated in Fig. 4. This is achieved by applying the slice-selection and readout gradient on the same axis, i.e., parallel to the direction of flow.

When incorporated into a cine gradient-echo pulse sequence this scheme permits the generation of multiple images, each pertaining to a particular, well-defined phase of the cardiac cycle (*20*). From the displacement of the bolus, the flow velocity can be

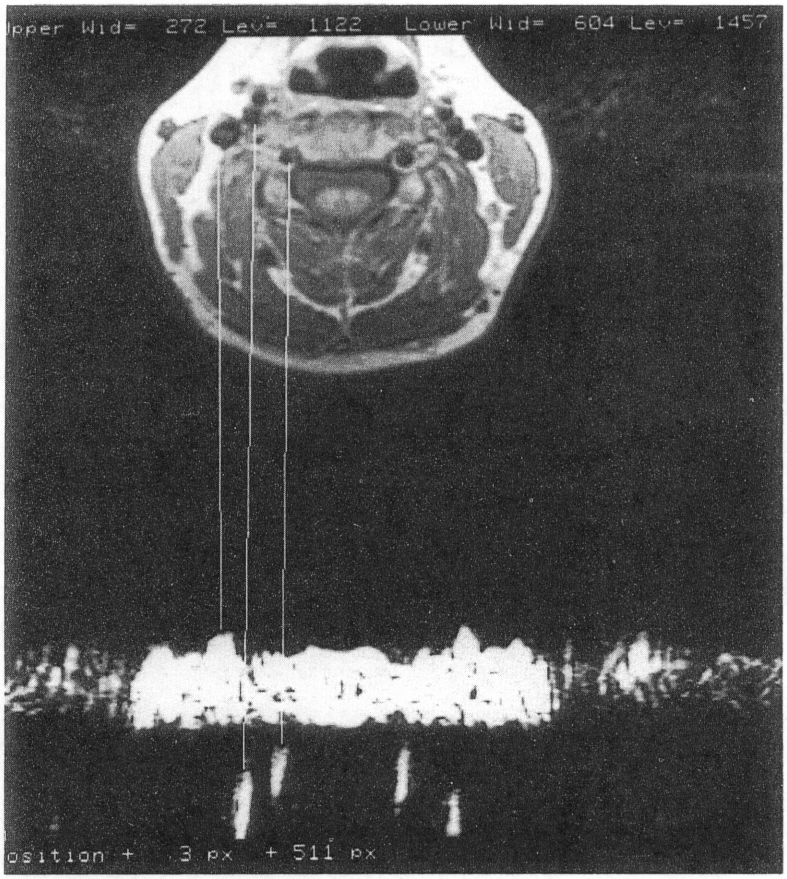

FIG. 5. Bolus tracking image obtained at the level of the common carotid arteries in a normal subject on a 1.5-T clinical imager (General Electric Signa), using the biplanar bolus tracking technique described in the text (bottom). The axial image was acquired at the same anatomic level and serves as a localizer relating functional (bolus displacement) and morphological (vessel position and size) information.

calculated as $v = d/\mathrm{TE}$, where d is the mean bolus displacement. Provided sufficient temporal resolution is available, velocity–phase diagrams can be constructed and such hemodynamic parameters as the systolic and diastolic flow velocity or their derivatives (acceleration) can be measured. A typical bolus tracking image, obtained by this method at the level of the common carotid arteries is shown in Fig. 5 (bottom), along with the pertinent axial image (top), serving as a localizer which relates the boli to the respective vascular anatomy.

In summary, time-of-flight effects are a widely observed phenomenon in MR imaging. Their manifestations are varied, depending on pulse sequence and pulse timing parameters used, vessel orientation, and flow characteristics, anatomic location, etc.

REFERENCES

1. L. E. CROOKS, C. M. MILLS, P. L. DAVIS, *et al.*, *Radiology* **144,** 843 (1982).
2. F. W. WEHRLI AND W. G. BRADLEY, *in* "Magnetic Resonance Imaging: Principles, Methodology and Applications" (F. W. Wehrl 1988.
3. J. P. FELMLEE AND R. L. EHMA
4. D. G. NISHIMURA, A. MACOV (1987).
5. G. T. GULLBERG, F. W. WEHRI
6. P. R. MORAN, R. A. MORAN, A
7. F. W. WEHRLI, J. R. MACFALL,
8. P. T. VALK, J. D. HALE, L. E. C
9. L. AXEL, *Amer. J. Roentgenol.*
10. G. T. GULLBERG, M. A. SIMON
11. JIA-HONG GAO, S. K. HOLLAN
12. P. E. VALK, J. D. HALE, L. E. HIGGINS, *Amer. J. Roentgen*
13. J. R. SINGER AND L. E. CROOK
14. F. W. WEHRLI, A. SHIMAKAWA
15. F. W. WEHRLI, A. SHIMAKAWA
16. J. HENNIG, M. MUERI, P. BRUN
17. D. A. FEINBERG, L. E. CROOKS,
18. K. SHIMIZU, T. MATSUDA, T. S
19. L. AXEL, A. SHIMAKAWA, J. R.
20. F. W. WEHRLI, J. LISTERUD, A
21. K. A. KRAFT, P. P. FATOUROS,

Applications" (F. W. Wehrli, D. Shaw, and H. B. Kneeland, Eds.), VCH Publishers, New York, 1988.
3. J. P. FELMLEE AND R. L. EHMAN, *Radiology* **164,** 559 (1987).
4. D. G. NISHIMURA, A. MACOVSKI, J. M. PAULY, AND S. M. CONOLLY, *Magn. Reson. Med.* **4,** 193 (1987).
5. G. T. GULLBERG, F. W. WEHRLI, A. SHIMAKAWA, AND M. A. SIMONS, *Radiology* **165,** 241 (1987).
6. P. R. MORAN, R. A. MORAN, AND N. KARSTAEDT, *Radiology* **154,** 433 (1985).
7. F. W. WEHRLI, J. R. MACFALL, L. AXEL, *et al., Noninvasive Med. Imaging* **1,** 127 (1984).
8. P. T. VALK, J. D. HALE, L. E. CROOKS, *et al., Amer. J. Roentgenol.* **146,** 931 (1986).
9. L. AXEL, *Amer. J. Roentgenol.* **143,** 1157 (1984).
10. G. T. GULLBERG, M. A. SIMONS, AND F. W. WEHRLI, *Magn. Reson. Imaging* **6,** 437 (1988).
11. JIA-HONG GAO, S. K. HOLLAND, AND J. C. GORE, *Med. Phys.* **15,** 809 (1988).
12. P. E. VALK, J. D. HALE, L. E. CROOKS, L. KAUFMAN, M. S. ROOS, D. A. ORTENDAHL, AND C. B. HIGGINS, *Amer. J. Roentgenol.* **146,** 931 (1986).
13. J. R. SINGER AND L. E. CROOKS, *Science* **221,** 654 (1983).
14. F. W. WEHRLI, A. SHIMAKAWA, J. R. MACFALL, *et al., J. Comput. Assist. Tomogr.* **9,** 537 (1985).
15. F. W. WEHRLI, A. SHIMAKAWA, T. GULLBERG, AND J. R. MACFALL, *Radiology* **160,** 781 (1986).
16. J. HENNIG, M. MUERI, P. BRUNNER, AND H. FRIEDBURG, *J. Comput. Assist. Tomogr.* **11,** 872 (1987).
17. D. A. FEINBERG, L. E. CROOKS, J. HOENNINGER, *et al., Radiology* **153,** 177 (1984).
18. K. SHIMIZU, T. MATSUDA, T. SAKURAI, *et al., Radiology* **159,** 195 (1986).
19. L. AXEL, A. SHIMAKAWA, J. R. MACFALL, *Magn. Reson. Imaging* **4,** 199 (1986).
20. F. W. WEHRLI, J. LISTERUD, AND P. CHAO, *Magn. Reson. Imaging* **7,** 195 (1989).
21. K. A. KRAFT, P. P. FATOUROS, D. Y. FEI, *et al., Magn. Reson. Imaging* **7,** 69 (1989).

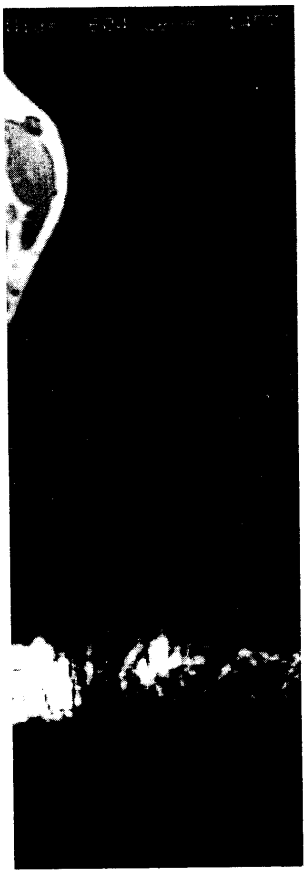

nmon carotid arteries in a normal subject planar bolus tracking technique described e anatomic level and serves as a localizer ssel position and size) information.

displacement. Provided sufficient iagrams can be constructed and diastolic flow velocity or their de- ıl bolus tracking image, obtained otid arteries is shown in Fig. 5 op), serving as a localizer which

bserved phenomenon in MR im- n pulse sequence and pulse timing cteristics, anatomic location, etc.

44, 843 (1982).
ce Imaging: Principles, Methodology and